Weierstraß-Institut

für Angewandte Analysis und Stochastik

Leibniz-Institut im Forschungsverbund Berlin e. V.

Stationary patterns of coherence and incoherence in two-dimensional arrays of non-locally coupled phase oscillators

Oleh Omel'chenko[1,2], Matthias Wolfrum[1], Serhiy Yanchuk[3], Yuri Maistrenko[2,4],

Oleksandr Sudakov[4]

[1] Weierstrass Institute
    Mohrenstr. 39
    10117 Berlin, Germany
    E-Mail: Oleh.Omelchenko@wias-berlin.de
            Matthias.Wolfrum@wias-berlin.de

[2] Institute of Mathematics
    National Academy of Sciences of Ukraine
    Tereshchenkivska Str. 3
    01601 Kyiv, Ukraine
    E-Mail: omel@imath.kiev.ua

[3] Institute of Mathematics
    Humboldt University of Berlin
    Unter den Linden 6
    10099 Berlin, Germany
    E-Mail: yanchuk@math.hu-berlin.de

[4] National Center for Medical and Biotechnical Research
    National Academy of Sciences of Ukraine
    Volodymyrska Str. 54
    01030 Kyiv, Ukraine
    E-Mail: y.maistrenko@biomed.kiev.ua
            saa@grid.org.ua

Abstract

Recently it has been shown that large arrays of identical oscillators with non-local coupling can have a remarkable type of solutions that display a stationary macroscopic pattern of coexisting regions with coherent and incoherent motion, often called *chimera states*. We present here a detailed numerical study of the appearance of such solutions in two-dimensional arrays of coupled phase oscillators. We discover a variety of stationary patterns, including circular spots, stripe patterns, and patterns of multiple spirals. Here, the stationarity means that for increasing system size the locally averaged phase distributions tend to the stationary profile given by the corresponding thermodynamic limit equation.

Recently, a new dynamical phenomenon has been reported that can be observed in arrays of non-locally coupled phase oscillators. Under specific conditions there are solutions that display a stable stationary pattern of coexisting coherent and incoherent motion in a population of identical oscillators. These solutions, called chimera states, have been first discovered in one-dimensional arrays with periodic boundary conditions [1], and have attracted considerable attention, bringing together the mathematical topics of synchronization in coupled oscillator systems and pattern formation.

Chimera states have up to now been observed in several types of coupled oscillator systems ranging from Kuramoto-like systems with various types of non-local interaction [2, 3, 4, 5, 6, 7, 8, 9, 10] to more complicated oscillators [11, 12, 13, 14] or inhomogeneous systems [15, 16, 6, 17, 18, 19]. Generally speaking, to observe chimera states the following ingredients have to be present in a system: First, the system has to represent a discrete medium, typically a large array of coupled units. This coupling has to be non-local, providing an interaction in a range that includes more than only next neighbors. Finally, there has to be a well tuned balance of attraction and repulsion between the oscillator phases that is typically achieved by a Sakaguchi phase lag parameter or a coupling delay. In addition to the careful choice of such a system structure with suitable parameters, it is necessary to provide appropriate initial conditions, since the classical chimera states typically coexist with the completely coherent (synchronized) state. This property distinguishes them clearly from classical Turing patterns, that emerge in a bifurcation, where the homogeneous state loses its stability with respect to a spatial modulation.

The motion in the incoherent region of a chimera state manifests itself as a spatially extensive deterministic chaos with a corresponding weakly chaotic Lyapunov spectrum [20]. In the thermodynamic limit of infinitely many oscillators with a macroscopic coupling structure, the incoherent motion turns into a statistically stationary behavior that is described by the macroscopic local mean field parameter. In this setting, the chimera states appear as spatially inhomogeneous equilibrium profiles.

Whereas, there is already an extensive literature about one-dimensional chimera states, the two-dimensional setting has received up to now much less attention. A first intriguing example

of a coherence–incoherence pattern in a two-dimensional array has been reported by Shima and Kuramoto [21] who presented a solution displaying a spiral wave of coherent oscillators with a region of incoherent motion in its core. This spiral chimera has then been further studied in [6, 22]. As a surprising fact, it occurs in a quite different parameter region than the classical one-dimensional patterns. Moreover it has been presented not for periodic boundary conditions, but for an unbounded domain, such that the coherent region is of infinite size. This is another striking difference to the classical one-dimensional chimera where the coherent domain is typically smaller than the incoherent one.

Independently from the above mentioned results, Kim et al. [23] have studied a similar system of coupled phase oscillators in a two-dimensional array with periodic boundary conditions. Using only random initial conditions, they observed patterns with several incoherent spiral cores occurring in a similar parameter region as the spiral chimera mentioned above. But these irregular multi-spiral patterns are typically not stationary; instead, the incoherent spots at the spiral cores show a slow motion that is caused by their mutual interaction and that may even lead to an annihilation of several incoherent spiral cores in a collision. The parameter region of the classical one-dimensional chimera also remained out of the scope of their study.
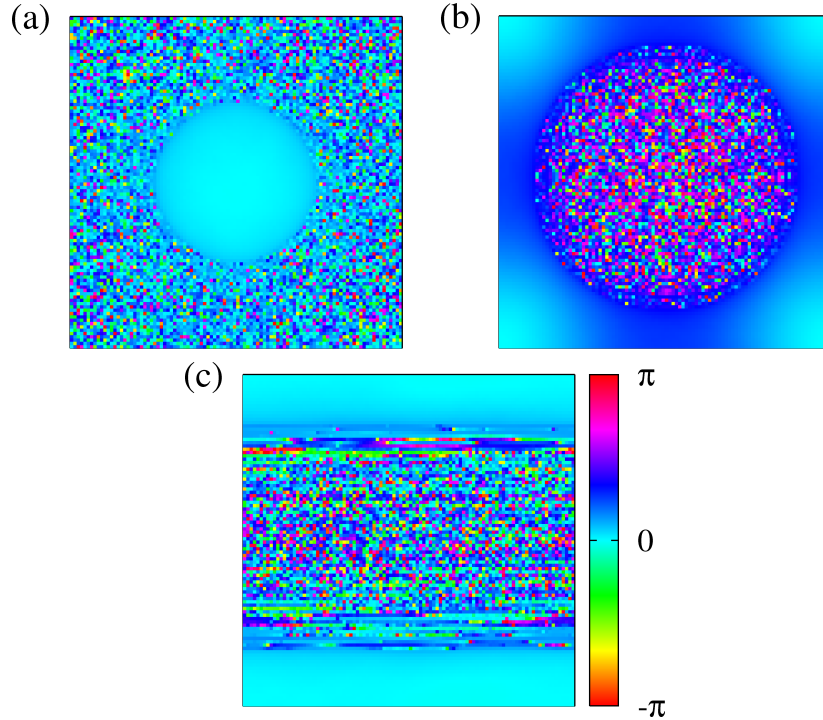

Figure 1: Snapshots of phase distributions Ψ_{jk} for trajectories of system (1) with $N = 100$, showing three different types of coherence-incoherence patterns. (a) Coherent spot. Parameters: $R = 44$, $\alpha = 1.52$. (b) Incoherent spot. Parameters: $R = 32$, $\alpha = 1.35$. (c) Stripe pattern. Parameters: $R = 40$, $\alpha = 1.44$.

In this paper, we present the two-dimensional counterparts of the classical one-dimensional chimera. We show a variety of spot and stripe patterns (see Fig. 1) with properties that resemble

those of the chimera states in one dimension and occur in a similar parameter regime. Our model is a two-dimensional array of $N \times N$ identical phase oscillators of Kuramoto-Sakaguchi type with phases $\{\Psi_{jk}(t)\}_{j,k=1}^{N}$ evolving according to

$$\dot{\Psi}_{jk} = \omega - \frac{1}{|B_R(j,k)|} \sum_{(m,n) \in B_R(j,k)} \sin(\Psi_{jk} - \Psi_{mn} + \alpha). \tag{1}$$

Both indices are considered modulo N, inducing a torus structure on the array. We take the natural frequency ω of all oscillators identical and hence it could be set to zero without loss of generality. The coupling range R, with $0 < R < N/2$, is used to define for every point (j,k) the circular neighborhood

$$B_R(j,k) := \left\{ (m,n) \ : \ (m-j)^2 + (n-k)^2 \leq R^2 \right\},$$

where distances $m - j$ and $n - k$ have to be calculated regarding the above mentioned torus structure of the array. The non-local interaction term in (1) is normalized by the number of points $|B_R(j,k)|$ in the neighborhood $B_R(j,k)$, and, finally, $\alpha \in (0, \pi/2)$ denotes the phase lag parameter. This particular setting is identical to that in [23] and has been mainly chosen for the reason of simplicity of numerical computations. However, we expect that any lattice system that is described by our thermodynamic limit equation (see Eq. (5)–(6) below) should display similar phenomena. Corresponding numerical experiments (not shown) for triangular or even irregular lattices confirm this. We also remark that coherence-incoherence patterns reported here can be found for different non-local coupling schemes with exponential or sinusoidal coupling functions, as have been used in [21, 6, 22].

Since chimera states are typically observed in coupled systems with large numbers of oscillators, the thermodynamic limit $N \to \infty$ becomes the most powerful tool for their investigation [1, 24, 25]. Indeed, with $N \to \infty$ and a macroscopic coupling range $r = R/N$ that tends to a constant, it provides a macroscopic description where the chimera states appear as stationary solutions revealing important macroscopic properties such as the size and shape of the coherent region and the averaged phase velocities of oscillators. To explain this limiting procedure in more detail, let us first rewrite system (1) in the equivalent form

$$\dot{\Psi}_{jk}(t) = \omega + \text{Im}\left(Z_{jk}(t)e^{-i\Psi_{jk}(t)}\right), \tag{2}$$

where

$$Z_{jk}(t) = \frac{1}{|B_R(j,k)|} \sum_{(m,n) \in B_R(j,k)} e^{i\Psi_{mn}(t)} e^{-i\alpha} \tag{3}$$

is the non-local mean field, given by the oscillators' positions on the unit circle averaged over the coupling range. Then we introduce for each oscillator Ψ_{jk} its normalized position

$$x_{jk} := (j/N, k/N) \in S = [0,1] \times [0,1] \subset \mathbb{R}^2.$$

With increasing N these positions densely fill the unit square. Following the approach of Pikovsky and Rosenblum [26], we may assume that for any point $x \in S$ the oscillators in a small vicinity of this point behave as a globally coupled sub-population. The collective behavior of the

sub-populations is then characterized by a local complex mean field $z(x,t)$ defined according to

$$z(x,t) := \lim_{N \to \infty} \frac{1}{|B_\delta^N(x)|} \sum_{(j,k) \in B_\delta^N(x)} e^{i\Psi_{jk}(t)}, \tag{4}$$

where $B_\delta^N(x) = \{(j,k) \ : \ |x - (j/N, k/N)| < \delta\}$ denotes a neighborhood of the point x. This is asymptotically correct in a thermodynamic limit where together with $N \to \infty$ the number of sub-populations as well as the number of points in the neighborhood $B_\delta^N(x)$ tend to infinity. Interpreting the space variable x as a sub-population index [26], we obtain an integro-differential equation for the effective dynamics of the local mean field $z(x,t)$

$$\frac{\partial z}{\partial t} = i\omega z(x,t) + \frac{1}{2}Z(x,t) - \frac{z^2(x,t)}{2}Z^*(x,t), \tag{5}$$

where

$$Z(x,t) = \frac{e^{-i\alpha}}{\pi r^2} \int\limits_{|x-y|<r} z(y,t)dy, \tag{6}$$

and the symbol $*$ denotes the complex conjugate. Recall that $x, y \in \mathbb{R}^2$ and the distance $|x-y|$ has to be taken on the torus $\mathbb{R}^2/\mathbb{Z}^2$. Note that (4) implies $0 \le |z(x,t)| \le 1$ for all x and t. For $|z(x,t)| = 1$ the oscillators around the point x are synchronized in phase, while $|z(x,t)| = 0$ corresponds to the local absence of phase synchronization. For a chimera state, $|z(x,t)| = 1$ identifies the coherent domain, while $|z(x,t)| < 1$ holds true in the incoherent domain.

In the framework of Eq. (5)–(6), a chimera pattern appears as a standing wave of the form

$$z(x,t) = \hat{z}(x)e^{i\Omega t},$$

where Ω is the common frequency of the coherent oscillators and $\hat{z}(x)$ is a complex-valued stationary profile. Note that, as a result of averaging procedure (4), $\hat{z}(x)$ is a continuous function of its argument $x \in S$. The coexistence of regions with coherent and incoherent motion is reflected by the fact that $|\hat{z}(x)| = 1$ and $|\hat{z}(x)| < 1$ in the corresponding regions. The motion of an oscillator in the coherent region is asymptotically given by

$$\Psi_{jk}(t) = \Omega t + \arg \hat{z}(x_{jk}). \tag{7}$$

In contrast to that, the phases of the oscillators in the incoherent region evolve irregularly and their motion can not be represented by a continuous profile.

Since any chimera pattern is a statistically stationary solution of system (1) it inherits the ergodicity property that the stationary local space-average $\hat{z}(x)$ can be approximated by the time-average of the single oscillator located at the corresponding point x. More precisely, choosing a reference oscillator Ψ_{coh} from the coherent region of the pattern we obtain for large N

$$\hat{z}(x_{jk})\hat{z}(x_{\text{coh}})^{-1} = \lim_{T \to \infty} \frac{1}{T} \int\limits_0^T e^{i\left(\Psi_{jk}(t) - \Psi_{\text{coh}}(t)\right)} dt, \tag{8}$$

where $x_{jk} = (j/N, k/N)$ and x_{coh} is the position of the reference oscillator Ψ_{coh}. Eq. (8) is useful for computing stationary mean field profile $\hat{z}(x)$ numerically. In Fig. 2 we illustrate the

4

limit $N \to \infty$. Panels (a)–(d) show the phase distributions for increasing N. Their local averages converge for $N \to \infty$ to the thermodynamic limit (panels (e), (f)). The corresponding stationary mean field profile $\hat{z}(x)$ has been evaluated according to (8). The sharp pattern structure for this time averaged quantities is a clear indication for the stationarity of the underlying coherence-incoherence pattern. In a similar way also the stationarity of the other patterns in Figs. 1 and 6 has been checked.

Numerical search for stationary patterns: As it has been pointed out for the classical one-dimensional chimeras ([1, 2]), such solutions exist only in a rather narrow parameter range and require suitably prepared initial data to find them in a numerical simulation.

For our initial search for stationary patterns, we performed massive parallel simulations using varying parameters α and R, and various types of initial conditions. We used initial data given by the formula

$$\Psi_{jk} = g(j/N, k/N)\xi,$$

where ξ is a random variable uniformly distributed within the interval $[-\pi, \pi]$ and $g(x_1, x_2)$ is a modulation function. For coherent and incoherent spots we used

$$g_{\mathrm{coh}}(x_1, x_2) = 1 - \exp(-10((x_1 - 0.5)^2 + (x_2 - 0.5)^2))$$

and

$$g_{\mathrm{incoh}}(x_1, x_2) = \exp(-15((x_1 - 0.5)^2 + (x_2 - 0.5)^2)),$$

respectively. For stripes we chose

$$g_{\mathrm{stripe}}(x_1, x_2) = sin^2(\pi x_1).$$

Our numerics are based on the Runge-Kutta solver DOPRI5 that has been integrated by a software for large nonlinear dynamical networks [27, 28], allowing for parallelized simulations with different sets of parameters and initial conditions. By visual inspection of the simulation data, we were able to find three types of stable stationary patterns in the parameter regime where the classical one-dimensional chimeras can be found: an incoherent spot in a coherent background and a coherent spot in an incoherent background, see Fig. 1 (a)–(c). Fig. 3 shows that incoherent spots (circles) appear for smallest values of $\alpha \approx 1.3$, followed by stripes (crosses) and coherent spots (diamonds) for α closer to $\pi/2$. Note that the regions partially overlap, which indicates the coexistence of patterns of different type.

Similarly to the classical one-dimensional chimera [2, 3], for all these patterns the relative size of the coherent region varies for changing parameters α and R. In Fig. 4 we show the two branches of coherent and incoherent spots, which appear for fixed $R = 36$ and varying parameter α. Panel (c) shows that for increasing α the relative number of coherent oscillators, given by the synchronization rate S, decreases monotonically. We display the biggest incoherent spot (a), which loses stability before it starts to interact with the boundary. Panel (b) then shows the biggest coherent spot. This Figure indicates in particular that there is no trivial transition regime between these two types of patterns.

The stripe patterns could be considered as a trivial extension of the well-known patterns in one dimension. However, their stability cannot be inferred from corresponding 1D results. Indeed,

5

for varying aspect ratio of the domain, the stability of the stripe patterns changes. In Figure 5 we show different examples that illustrate how the stability is influenced by the length of the stripe. In panel (a), we have chosen parameter values outside the stability region for the square domain (given by blue crosses in Fig. 3). Anyhow, for a sufficiently short length, the stripe is stable. This corresponds to the fact that also in 1D there is a corresponding stable pattern. In panels (b) and (c), we have chosen parameter values inside the stability region for the square domain. For a domain of 120×100, the stripe pattern is still stable (b). For larger aspect ratio, an instability with respect to a longitudinal modulation of the stripe width appears. This instability is subcritical, and panel (c) shows only a snapshot of a transient starting with a stripe initial condition, but converging to a state without a chimera pattern.

In addition, for much smaller values of α and R we found a stable configuration of four spirals (see Fig. 6 (a)). Note that the stationary pattern with a single spiral in an unbounded domain, presented in [22] does not exist for periodic boundary conditions. However, as for spiral waves in reaction-diffusion systems, an even number of counter-rotating spirals can satisfy periodic boundary conditions. Fig. 6 (b) shows that the stationary spiral pattern (cf. Fig. 6) can be observed in a rather distant region of the parameter space.

The numerical complexity to determine these regions by simulations is extremely high. We performed simulations of system (1) with $N^2 = 10,000$ variables over a time intervals of length $T = 1000$ for various initial conditions and parameters α and R. In principle, the stability boundaries of the stationary patterns could be investigated more efficiently by a linear stability analysis of the thermodynamic limit equation (5), subject to a numerical path-following approach. However, due to the presence of continuous spectrum for the corresponding integral operator (see [20] for details), standard algorithms fail here and further theoretical investigations are required.

In addition to the stationary patterns that are presented here, we observed also indications for various types of oscillatory and intermittent behavior. In particular, at the stability boundaries we numerically observed a wealth of interesting dynamical phenomena. Moreover, for similar values of α as in Fig. 3(a) and considerably smaller R, we cannot exclude the possible existence of patterns with multiple stripes or spots. But seemingly their stability is very sensitive to the proper choice of parameters and initial conditions, such that we were not able to detect them within this study.

References

[1] Y. Kuramoto and D. Battogtokh, Nonlinear Phenom. Complex Syst. **5**, 380 (2002).

[2] D. M. Abrams and S. H. Strogatz, Phys. Rev. Lett. **93**, 174102 (2004).

[3] D. M. Abrams and S. H. Strogatz, Int. J. Bif. and Chaos **16**, 21 (2006).

[4] G. C. Sethia, A. Sen, and F. M. Atay, Phys. Rev. Lett. **100**, 144102 (2008).

[5] C. R. Laing, Chaos **19**, 013113 (2009a).

[6] C. R. Laing, Physica D **238**, 1569 (2009b).

[7] O. E. Omel'chenko, M. Wolfrum, and Y. L. Maistrenko, Phys. Rev. E **81**, 065201 (2010a).

[8] M. Wolfrum and O. E. Omel'chenko, Phys. Rev. E **84**, 015201 (2011).

[9] W. S. Lee, J. G. Restrepo, E. Ott, and T. M. Antonsen, Chaos **21**, 023122 (2011).

[10] C. R. Laing, Physica D **240**, 1960 (2011).

[11] H. Sakaguchi, Phys. Rev. E **73**, 031907 (2006).

[12] Y. Kawamura, Phys. Rev. E **75**, 056204 (2007).

[13] G. Bordyugov, A. Pikovsky, and M. Rosenblum, Phys. Rev. E **82**, 035205 (2010).

[14] I. Omelchenko, B. Riemenschneider, P. Hovel, Y. L. Maistrenko, and E. Scholl, Phys. Rev. E (2012).

[15] O. E. Omel'chenko, Y. L. Maistrenko, and P. A. Tass, Phys. Rev. Lett. **100**, 044105 (2008).

[16] O. E. Omel'chenko, Y. L. Maistrenko, and P. A. Tass, Phys. Rev. E **82**, 066201 (2010b).

[17] D. M. Abrams, R. Mirollo, S. H. Strogatz, and D. A. Wiley, Phys. Rev. Lett. **101**, 084103 (2008).

[18] E. A. Martens, Phys. Rev. E **82**, 016216 (2010).

[19] C. R. Laing, Phys. Rev. E **81**, 066221 (2010).

[20] M. Wolfrum, O. E. Omel'chenko, S. Yanchuk, and Y. L. Maistrenko, Chaos **21**, 013112 (2011).

[21] S. I. Shima and Y. Kuramoto, Phys. Rev. E **69**, 036213 (2004).

[22] E. A. Martens, C. R. Laing, and S. H. Strogatz, Phys. Rev. Lett. **104**, 044101 (2010).

[23] P.-J. Kim, T.-W. Ko, H. Jeong, and H.-T. Moon, Phys. Rev. E **70**, 065201(R) (2004).

[24] E. Ott and T. M. Antonsen, Chaos **18**, 037113 (2008).

[25] E. Ott and T. M. Antonsen, Chaos **19**, 023117 (2009).

[26] A. Pikovsky and M. Rosenblum, Phys. Rev. Lett. **101**, 264103 (2008).

[27] R. I. Levchenko, O. O. Sudakov, and Y. L. Maistrenko, in *Proc. 17th International Workshop on Nonlinear Dynamics of Electronic Systems, June 2009, Rapperswille, Switzerland* (2009), pp. 34–37.

[28] A. O. Salnikov, I. A. Sliusar, O. O. Sudakov, O. V. Savytskyi, and A. I. Kornelyuk, in *Proc. IEEE International Workshop on Intelligent Data Acquisition and Advanced Computing Systems: Technology and Applications, 21-23 September 2009, Rende (Cosenza), Italy* (2009), pp. 237–240.
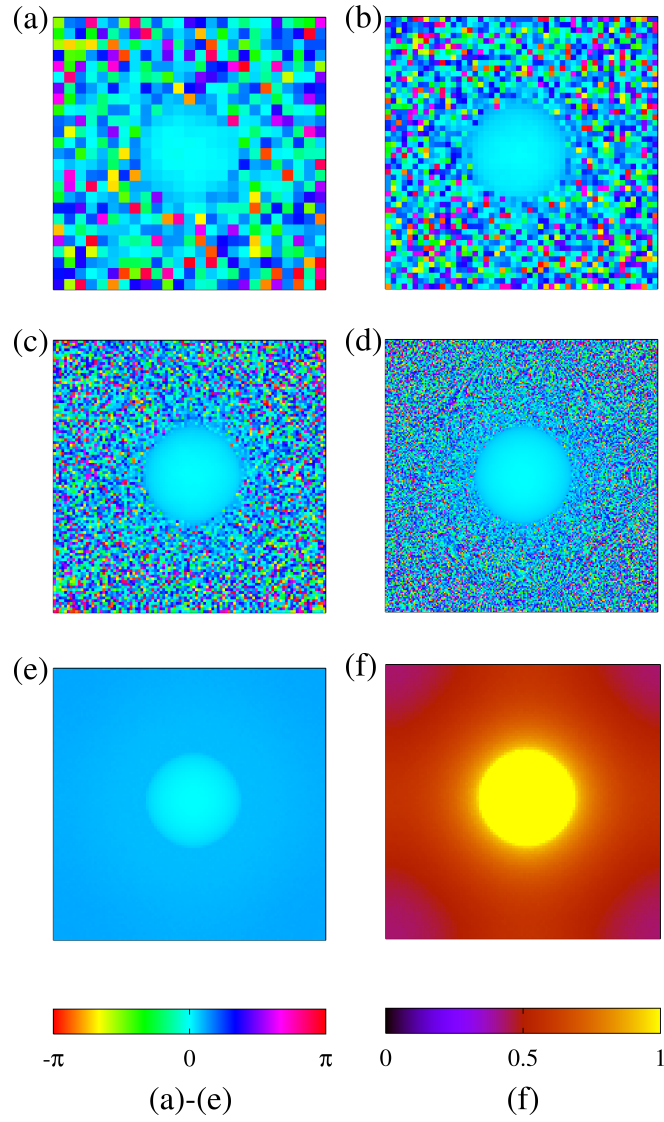
Figure 2: Coherent spot pattern with $R/N = 0.4$, $\alpha = 1.54$ for increasing N; Snapshots of phases Ψ_{jk}: (a) $N = 25$, (b) $N = 50$, (c) $N = 100$, (d) $N = 200$; thermodynamic limit profile: (e) $\arg(\hat{z}(x))$, (f) $|\hat{z}(x)|$.
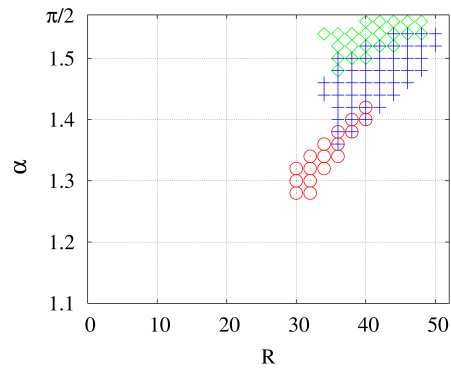
Figure 3: Parameter regions, where different types of stable stationary patterns from Fig. 1 have been observed in system (1) with $N = 100$: incoherent spots (circles), stripes (crosses), coherent spots (diamonds).
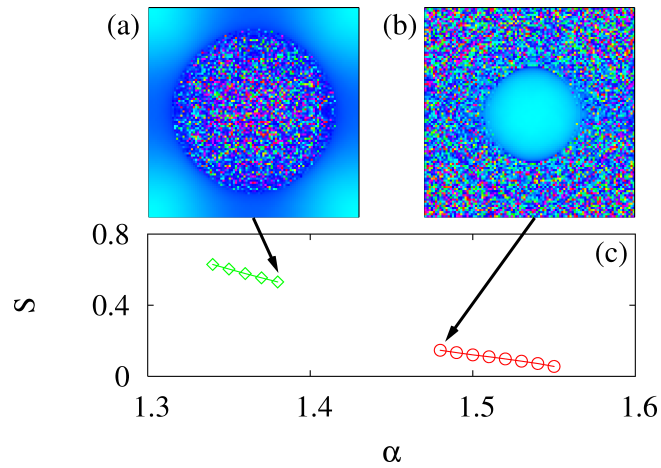

Figure 4: (c): Synchronization rate S for stable incoherent spots (circles) and coherent spots (diamonds) observed in system (1) with $N = 100$ and $R = 36$ and varying α. Panels (a) and (b) show the biggest incoherent spot and the biggest coherent spot.
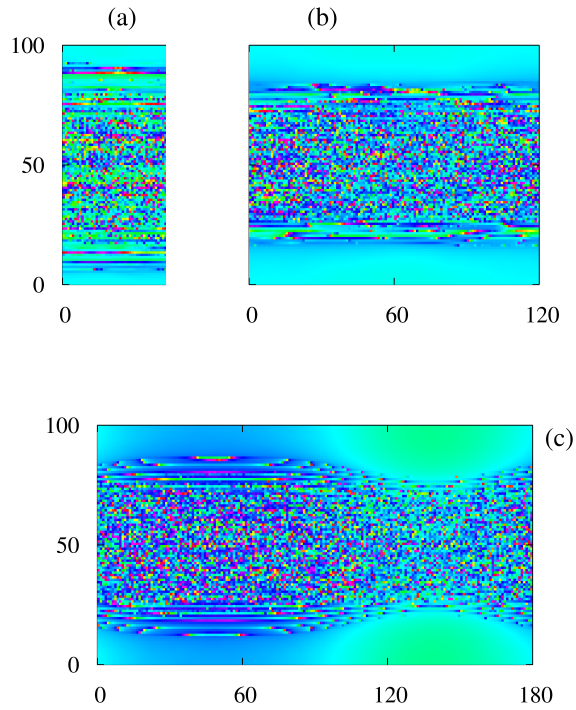
10

Figure 5: Stripe patterns for different aspect ratio of the domain: (a) stable stripe for $\alpha = 1.54$, $R = 36$ in a domain of 50×100; (b) stable stripe for $\alpha = 1.44$, $R = 40$ in a domain of 120×100; (c) unstable stripe for $\alpha = 1.44$, $R = 40$ in a domain of 180×100 (snapshot of transient, starting from a stripe initial condition).
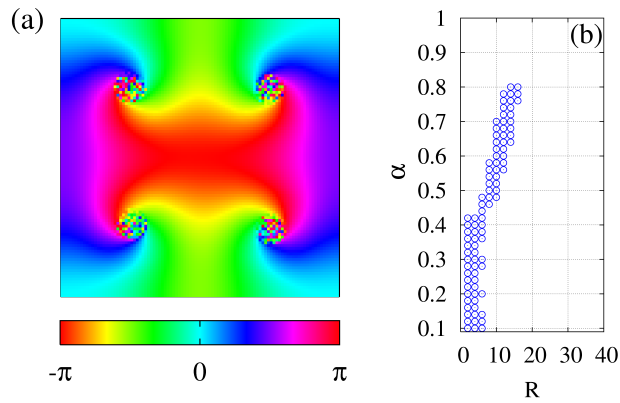

Figure 6: Stationary pattern of four spiral waves with incoherent core. (a) Snapshot of phases Ψ_{jk}. Parameters: $N = 100$, $R = 10$, $\alpha = 0.60$. (b) Parameter region, where the pattern has been observed.